Development of a Remaining Useful Life Model for Reinforced Concrete Beams subjected to High-Cycle Fatigue

June 6, 2021

Abstract

Purpose: Failure of a critical reinforced concrete beam due to fatigue can have severe safety and production consequences, and preventative repair/replacement of such a beam is expensive. It would therefore be beneficial if repair/replacement can be done based on an accurately and conservatively predicted Remaining Useful Life (RUL). The purpose of this paper is to develop such a model.

Design/methodology/approach: Condition based maintenance is a maintenance approach that uses empirical/analytical models and a measurable condition to predict remaining useful life. The P-F curve (condition-life) is a useful tool that can aid in making these decisions. A model to create a P-F curve is developed using rebar fatigue test results (in the form of an S-N curve) and the Palmgren-Miner law of damage accumulation. A Monte Carlo simulation with statistical distributions is employed to provide confidence levels of RUL outputs.

Findings: An example of how the model can successfully be used in practice is shown in this paper and a sensitivity study is performed leading to conclusions being drawn with regard to damage tolerant design considerations.

Originality/value: If a critical reinforced concrete beam fails due to fatigue can have serious consequences. This paper develops a model to help base repair/replacement decisions based on accurately and conservatively predicted Remaining Useful Life (RUL). Financial and safety benefits would be gained if this model would be used in practice.

1 Introduction

Reinforced concrete (RC) is a composite material that exploits the advantages of concrete and steel, and mitigates their respective disadvantages. The advantages of concrete are that it is easily molded into any shape, has a high compressive strength, and is relatively cheap. However, concrete has a low tensile strength and cracks easily. The tensile strength is improved by the addition of steel reinforcement. So, steel and concrete can effectively be combined to build relatively cheap structural elements with high strength and flexible uses (Guo, 2014, p. 2). Additionally, concrete also covers the steel to isolate it from the corrosive environment. Figure 1

shows the side and sectional view of a simply supported beam of length L, breadth b, height h, with two rebars and load P applied at two points with span s between them. The position of the two reinforcements and the section view are also shown. In this configuration, the load causes bending putting the reinforcements at the bottom in tension and concrete at the top in compression.

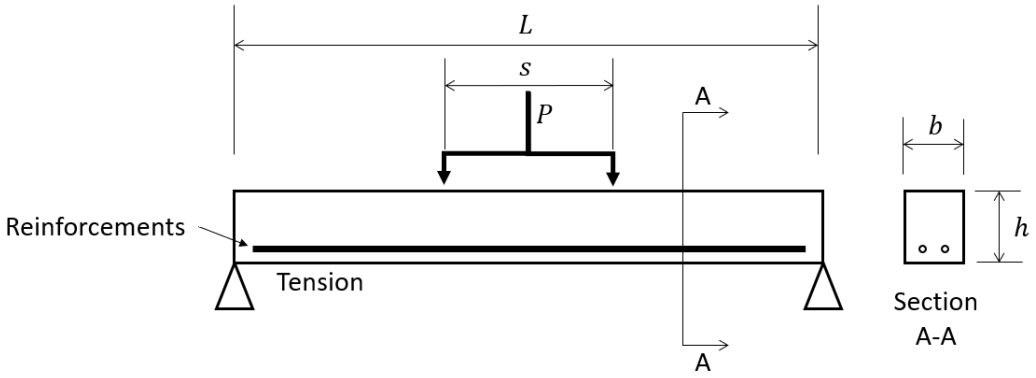

Figure 1: Side and sectional view of a simply supported beam of length L, breadth b, height h, with two rebars and load P applied at two points with span s between them

Reinforced concrete structures form the backbone of industrial, commercial and civil infrastructure. It is obvious and universally accepted that structural integrity is established through the application of sound design practices and sustained through the application of sound maintenance practices. Due to the relatively long design lives and damage tolerant nature of RC structures, in comparison to eg. machine structures and components, they have not been high priority items from a maintenance point of view. However, much infrastructure is ageing and, in many instances, already past these intended design life.

Ageing failure mechanisms for structures include corrosion, wear and fatigue. The most prevalent of these mechanisms in relation to RC structures, namely corrosion, is a widely explored field, especially for coastal structures (Yi et al., 2011 and Chen & Alani, 2013). Fatigue and wear, on the other hand, are not so widely explored so it is an avenue for further research. Also, the understanding of fatigue in cementitious composites (such as reinforced concrete) is still lacking (Lee & Barr, 2004). The present study therefore focusses on the *fatigue* mechanism.

Fatigue is the accumulation of damage due to fluctuating stress and can cause failure even if the stress is below the yield strength of the material. The risk of fatigue failure has historically been addressed during design by applying large safety factors, or more recently by defining the dynamic loads in combination with the required life, as a limit state (limit state is a design method covered later). However, in either case, structures subjected to significant high-cycle dynamic loading, will have finite design lives, which, when exceeded, introduce the risk of failure.

Examples of cases where reinforced concrete structures are subjected to fatigue include bridges, cranes, stacks, crusher structures, and off-shore structures where traffic, movement of the crane, wind loads, tipping/delivery of ore, and waves are the respective causes of cyclical loading. Highway bridges, for example, have design lives of 120 years during which time up to 7×10^8 cycles of traffic induced stress may be applied. Offshore structures can have operational lives of 30 years during which time they will be subjected to more than 1×10^8 cycles of stress caused by the action of waves (Tilly, 1979).

For such structures, the risk of failures caused by ageing failure mechanisms can be high because the consequences of failure could include significant collateral damage, as well as injury or death.

Sound maintenance must be done to ensure the safety and integrity of structures and to avoid plant downtime and cost of repair.

Maintenance approaches are generally divided into two categories: *corrective* and *preventive* maintenance (Prajapati et al., 2012). Corrective maintenance involves merely running a component to failure and replacing or repairing after failure. This is a reactive tactic, also known as run-to-failure. For components with a more severe consequence of failure, preventive maintenance tactics are required. Preventive maintenance involves having a deeper understanding of the component to do predictive calculations. Preventive maintenance tactics include time based maintenance (TBM), when a component is replaced/repaired at a specific, predetermined time in its life, disregarding the condition of the specific component and usage based maintenance (UBM), when the repair/replacement depends on a chosen parameter such as tonnes, rotations or kilometres. Time and usage based maintenance are based on historical trends. When doing time or usage based maintenance, useful life could be lost due to premature repair or replacement and in the case of RC structures, economic considerations often precludes these approaches.

Condition based maintenance (CBM), on the other hand, recommends maintenance actions based on information collected via condition monitoring (Campbell & Reyes-Picknell, 2015). The advantage of CBM is that there is less loss of useful life due to premature action. However, a quantification of the Remaining Useful Life (RUL) of a structural member, based on measurable condition parameters, is needed to implement CBM. The present study focusses on the development of a Remaining Useful Life model for reinforced concrete beams subjected to high-cycle fatigue.

2 Theory and Principles

2.1 Condition based maintenance

Condition based maintenance (CBM) is a maintenance approach that aims to minimize failures and wasted life by making maintenance decisions based on the condition of a physical asset, such as machines or a structural component. An example of this is the familiar decision about when to charge a cellphone based on information about the remaining battery life.

A well-known curve that describes the behaviour of the condition towards failure is called the P-F curve. Figure 2 shows an example of a P-F curve. The P-F curve is a plot of the measured condition (such as crack length) against the life (such as cycles). Deteriorating condition, caused by ageing mechanisms such as fatigue, wear and corrosion, is depicted by a descending trend on the vertical axis. The curve shows the point of potential failure (P), where defects are detectable. After the "P" point has been reached, the component's condition will start to deteriorate until failure (F) (or loss in function) occurs (Blann, 2013). Failure (or functional failure) is a chosen condition representing what lowest tolerable condition. The time taken from potential failure to degrade to failure is the P-F interval. The shape of this curve can either be determined analytically or empirically (Prajapati et al., 2012).

The P-F interval is of most importance from a maintenance point of view. Inspection interval optimisation, planning and decisions are based on this interval. A longer P-F interval is more preferable (Blann, 2013). A few P-points can exist after the first P that indicate milestones between the P and F point (for instance, showing when inspections were/should be done).

The P-F curve represents the trend of the condition as it approaches failure (Wessels, 2010).

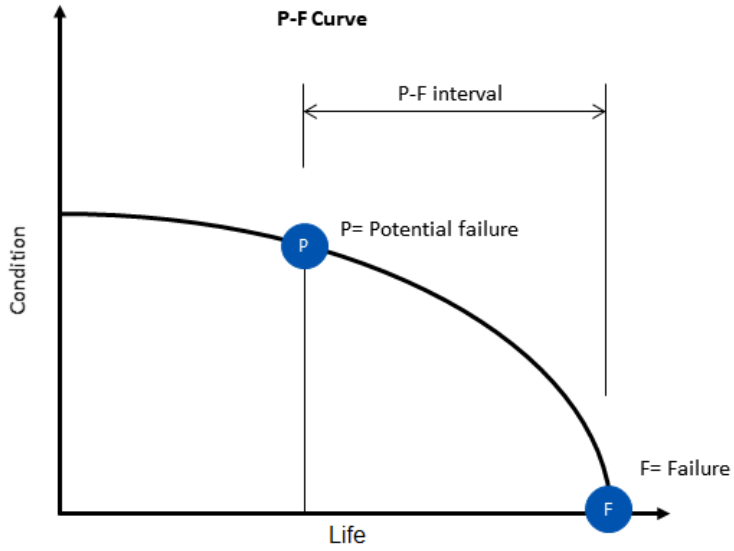

Figure 2: An example of a P-F curve

The P-F curve can only be created for a component with an ageing mechanism of failure i.e. when the condition of a component degrades over time, and the P-F curve would only be useful if the evidence of failure is measurable (Moubray, 1991, p. 116). The condition of the P-F curve may be normalised, defining a condition of one as meaning new and zero as failure condition. This is beneficial if different conditions of different components need to be compared or trended together. The shape of a P-F curve is often determined analytically (such as with the Paris law of crack growth (Paris et al., 1961)) and can often be a power law, meaning it takes an exponential shape.

The P-F curve may be used to determine the Remaining Useful Life (RUL). The P-F curve gives the whole trend of the condition towards failure, and the RUL is determined by looking at the current condition and calculating the remaining life.

An example of CBM application is engine diagnostics based on monitoring the metal content in engine oil (Wang et al., 2012). In this example, the failure mechanism is wear of the engine and the measured condition is metal content in the oil. A P-F curve could be developed based on lab experiments to determine the P-F interval. An overhaul of the engine should be done when a specific metal content is reached.

2.2 Fatigue of reinforced concrete beams

Structures that were designed correctly (according to a code such as SANS 10100-1:2000 or BS 8110-1:1997) will seldom fail due to static loading. The cause of such a failure would probably be overloading. However, a repeated/cyclical load acting on a structure can cause accumulation of damage, such as crack propagation, that can lead to fatigue failure.

A common way to present experimental results of fatigue tests is the S-N curve. The stress-life (S-N) method is an empirical method that dates back to Wohler in 1860 where a simplified equations such as Basquin's power law (see Equation 1) is formulated by fitting it on test data (Pugno et al., 2006). The test data are recorded failures. "Life" (N) could be operating hours, or load cycles. The present study will always use N to be cycles. On a log-log scale, Basquin's

equation gives a straight line,

$$N = C(\Delta\sigma)^m \tag{1}$$

where C & m are the shape factors, and $\Delta\sigma$ is stress range.

Figure 8 is an example of an S-N curve. One can do a best fit on the data using Basquin's equation, then that line would be the mean of the data, which could be useful in some cases. But if one knows how spread out the data is, statistical principles can be applied to give more accuracy within a certain confidence interval.

Numerous S-N curves for rebar and RC beams exist, such as presented by Nagesh & Rao (2016). Table 1 gives the relationships between number of cycles N and stress range $\Delta\sigma$ from various authors. The mean cycles to failure at an arbitrary stress of 257 MPa is given for each equation and the different S-N curves are shown in Figure 3.

Table 1: Fatigue life prediction equations

Author	**Equation**	**N @ 257 MPa**
BS 7608 (2014)	$\log N = 14.0342 - 3.5 \log \Delta\sigma$	397 589
Helgason et al. (1976)	$\log N = 6.969 - 0.00555\Delta\sigma$	348 859
Tilly & Moss (1982)	$N = 0.75 \times 10^{27}\Delta\sigma^{-9}$	153 342
CEB-FIP Model Code (2010)	$N = 4.0841 \times 10^{17}\Delta\sigma^{-5}$	364 276
Papakonstantinou et al. (2001)	$\log N = 6.677 - 0.00613\Delta\sigma$	126 354
Tilly (1979)	$\log N = 27.7 - 8.858 \log \Delta\sigma$	2 253 265

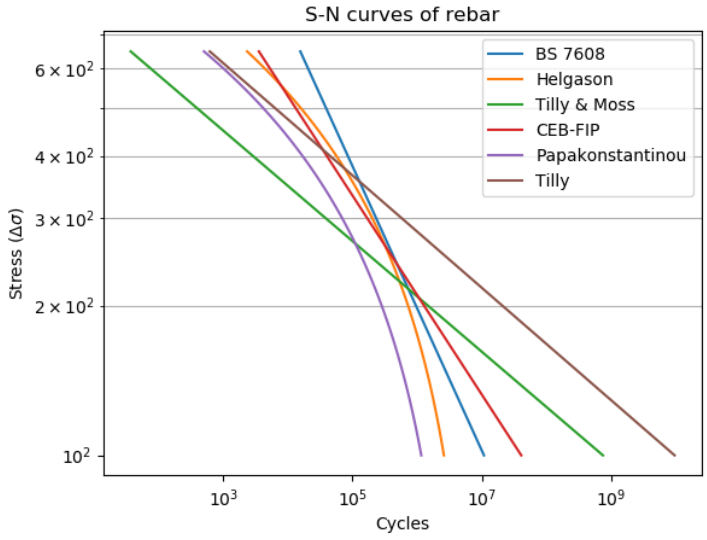

Figure 3: S-N Curves of RC beams from many authors

The S-N curve that will be used for rebar during this study is from Tilly (1979), because he gave the spread of his data. However, it is important to note that any of these S-N curves could have been used. Ideally, one would use experimental data of the specific batch of rebars used. The equation for Tilly's mean line is:

$$\log N = \log 27.7 - 8.858 \log \Delta\sigma \tag{2}$$

While the equation for Tilly's 95.45 percentile line is:

$$\log N = \log 27.7 - 8.858 \log \Delta\sigma + 2 \times SD \tag{3}$$

where $SD = 0.047$.

2.3 Flexural cracks as a condition of failure

The benefit of having a P-F curve based on the flexural crack is that it is external, so can be easily measured or otherwise a clip gauge can be installed.

When the tensile stress in the concrete reaches its modulus of fracture, the concrete will start cracking. As the crack propagates, the stress in the steel and concrete increases. Under service loads, flexural members will normally be in this region. An exaggeration of this cracked state is illustrated in Figure 4.

Flexural cracking is a likely occurrence and it does not necessarily detract from the load bearing integrity of the structure (Carino & Clifton, 1995), because the concrete was not intended to contribute to the tensile resistance during the design. Flexural cracks as a condition for failure have been investigated and presented previously by Jokubaitis et al. (2013).

The issue that Jokubaitis et al. aimed to address was to determine whether the external loads cause the tensile reinforcement to yield by looking at the flexural cracks. Yielding of the tensile reinforcement, in their case, was treated as the start of failure. The state of tensile reinforcement of flexural reinforced concrete structures was examined by observing the properties of the flexural cracks. They applied fracture mechanics to determine the actual damage to the structure by knowing only the measured height of the flexural crack.

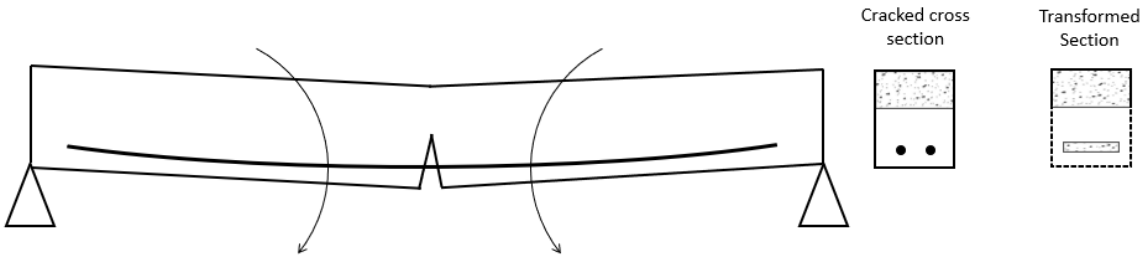

Figure 4: Side and sectional view of a RC beam subjected to Flexural Bending in a cracked state. The transformed steel area is also shown.

2.4 Examples of reinforced concrete beam life predicting models

Rocha & Brühwiler (2012) suggests a method to predict fatigue life of reinforced concrete bridges using Fracture Mechanics. In summary, Paris' law was used to model the crack growth in the rebars. The constant values (C, m) were taken from other literature and a conservative initial crack size was assumed. Using this method, they concluded that the beam in their case study is safe with respect to the current and future loads.

This method cannot be used for CBM because it models the fracture mechanics of the rebars, but the rebars are embedded inside the concrete, so it would be difficult to monitor the crack size. This method would be useful if TBM is to be applied.

Similarly, Guo et al. (2019) suggest a method of predicting corrosion accelerated fatigue life of a RC beam. They assume that corrosion creates an initial crack in the reinforcement and then also uses fracture mechanics to calculate the crack growth. In this case, measuring the condition is also difficult because the rebars are embedded in the concrete.

The present study aims to develop a method of predicting the life of RC beams by measuring the external concrete crack depth.

3 Development of a P-F curve for reinforced concrete beams

This section covers the development of a P-F curve for RC beams with fatigue as the ageing mechanism and flexural crack depth as the condition parameter. The curve is not deterministic but includes a random number of cycles to failure. The model is based on a curve of crack growth as a function of load cycles. Inverting and normalising this curve to show condition as a percentage produces a P-F curve.

The curve is proposed based on the following assumptions: the rebars fail sequentially (instead of all at once), flexural crack depth can be used as a measurable condition of failure, and the flexural crack grows uniformly over the width of the section of the beam. It has previously been reported that the rebars in a RC beam that is subjected to fatigue fail sequentially (JSCE 2007, p. 236) and Jokubaitis et al. (2013) previously used crack depth as a condition for failure. The first 2 assumptions are thus reasonable assumptions. The last assumption is a limitation of the model.

Figure 5 shows a graph of concrete crack growth over number of load cycles of a RC beam with four rebars.

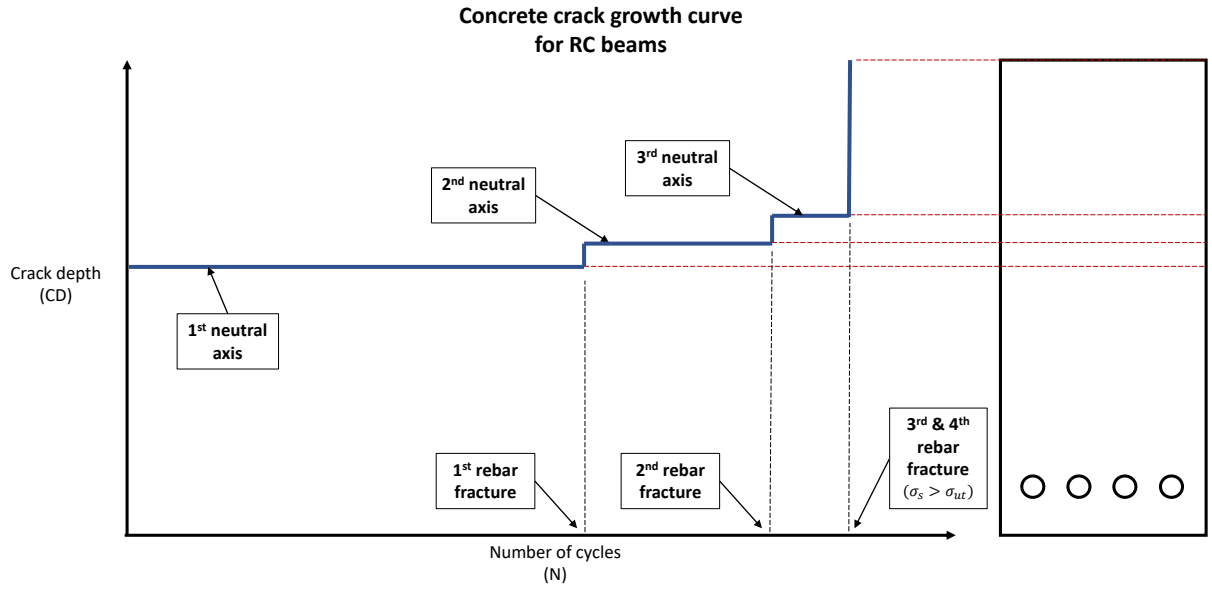

Figure 5: The proposed concrete crack growth curve for a RC beam with four rebars.

Once the load starts being applied, a concrete crack forms instantly to the depth of the neutral axis (NA) where the concrete at the top is in compression and the rebars are in tension.

The NA is calculated by using the proportional sum of areas as in Equation 4:

$$NA = \frac{y_1 A_1 + y_2 A_2}{A_1 + A_2} \tag{4}$$

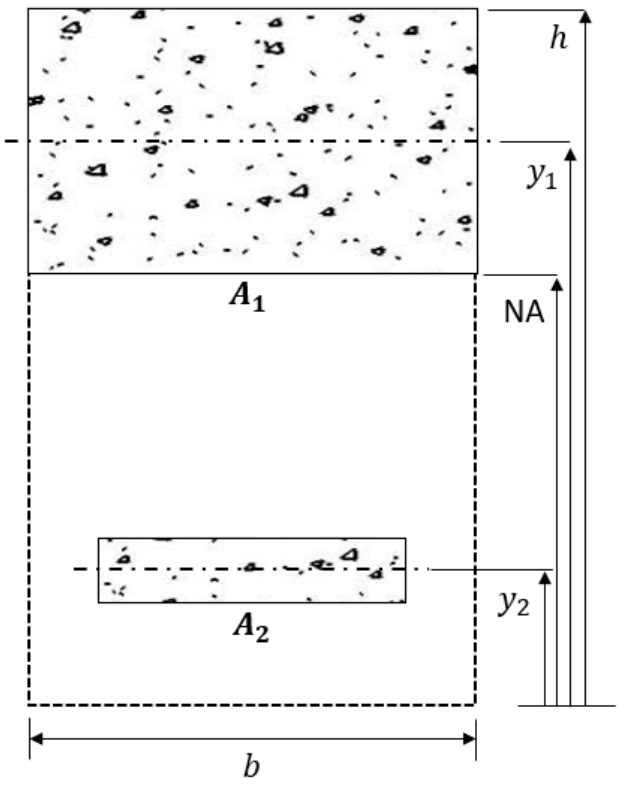

Figure 6: The section view of a beam with transformed steel area.

Where y_2 is the height of the rebars from the bottom (See Figure 6),

$$A_1 = b(h - NA) \tag{5}$$

And,

$$A_2 = num \times \frac{E_s}{E_c} \times \frac{\pi D^2}{4} \tag{6}$$

With, E_s is the modulus of elasticity of the steel rebars (normally around 200 GPa), E_c is the modulus of elasticity of the concrete (normally around 25 GPa), D is the diameter if the rebars, and num is the number of rebars. Lastly,

$$y_1 = NA + (h - NA)/2 \tag{7}$$

NA can be solved by substituting Equation 5, 6, 7 and y_2 into Equation 4.

The rebars experience tension and the concrete compression with each load cycle. The crack will stay at this depth until one of the rebars fractures due to fatigue. Then, the concrete crack will grow to a new neutral axis because of the decrease in steel area (A_2).

Again, the rebars will fatigue, but this time at a higher stress. When the next rebar fractures, the crack will grow to a new neutral axis. The rebars will then, again, fatigue at an even higher stress until a rebar fractures. After failure of the third rebar, the entire beam will fail because the stress will be above the ultimate tensile strength of the rebars.

This is the case for a beam with four rebars, however, the number of times the concrete crack grows to a new neutral axis depends on the number of rebars.

To create a P-F curve from this crack growth graph, the crack depth on the y-axis would just be normalised to a percentage by taking $condition = 1 - \frac{NA}{h}$.

The point of potential failure ("P") is reached when the first rebar fractures. Failure ("F" point) is reached when the crack grows through the beam. The P-F interval is, thus, defined as from 1st rebar failure to total beam failure. Maintenance decisions (such as interval of inspection and when to replace) are made within this interval.

The methodology that was followed to create these graphs with a computer model is outlined in the program flowchart in Figure 7 and is discussed in detail in Sections 3.1 - 3.5.

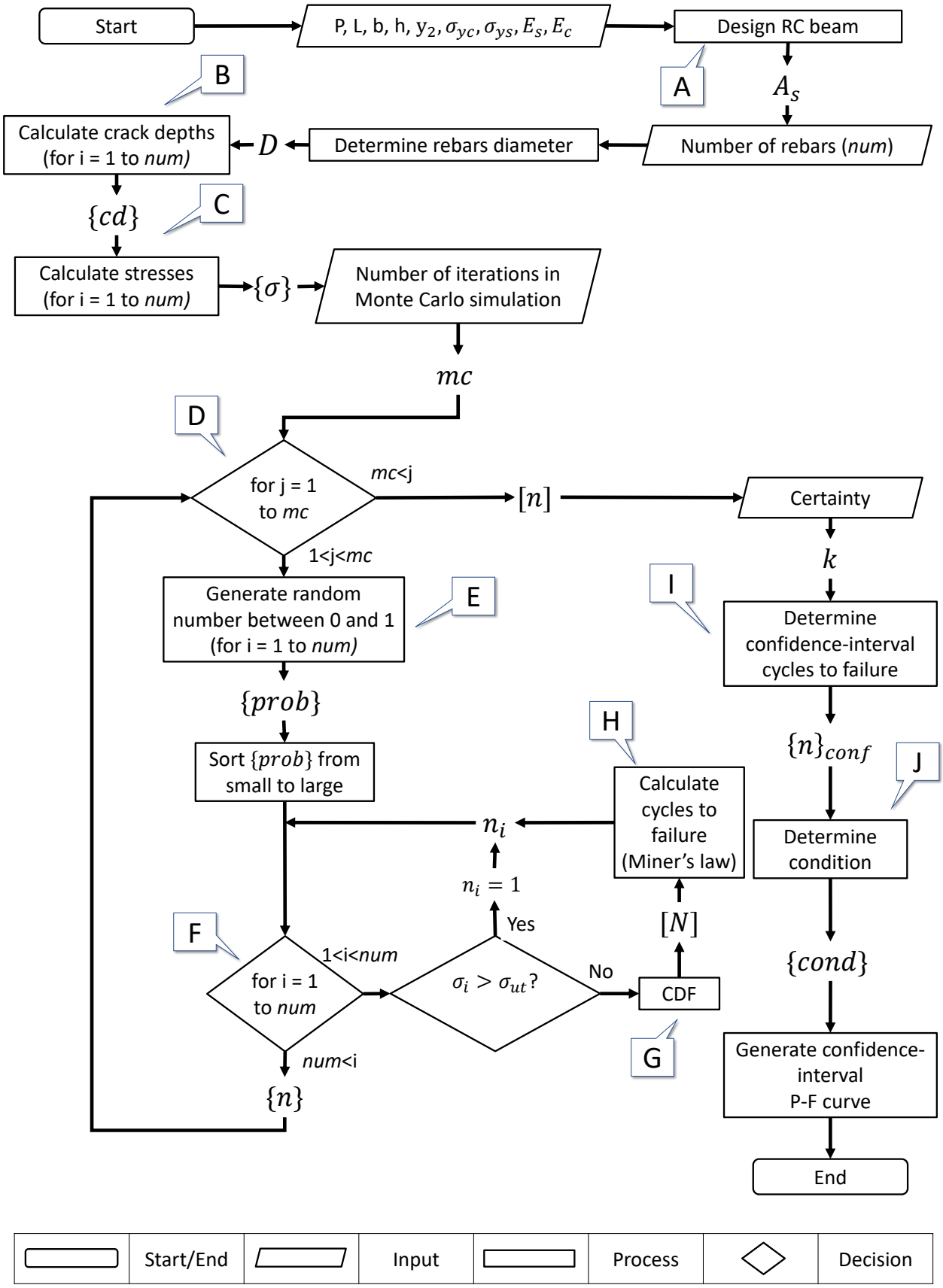

Figure 7: Program flowchart to create a P-F curve for a cyclical loaded reinforced concrete beam.

3.1 Design RC beam (A)

The design of a RC beam is done using the Limit State Design method. The required reinforcement area of the beam is calculated by using Equation 8, as given by Mosley & Bungey (1990) for a singly reinforced beam.

$$A_s = \frac{M_{max}}{0.87\sigma_{ys}z} \tag{8}$$

Where σ_{ys} is the yield strength of the rebars, M_{max} is the maximum bending moment caused by the applied force, and z is the lever arm between the resultant forces in the steel and the concrete, calculated using:

$$z = (h - y_2)(0.5 + \sqrt{0.25 - \frac{K}{0.9}}) \tag{9}$$

With,

$$K = \frac{M_{max}}{b(h - y_2)^2\sigma_{yc}} \tag{10}$$

Where σ_{yc} is the characteristic material strength of the concrete (normally between 20 and 40 MPa).

The required rebar diameter (D) is determined by using the defined number of rebars (num) as follows:

$$D = \sqrt{\frac{4A_s}{\pi \times num}} \tag{11}$$

Alternatively, if D is fixed, the required number of rebars (num) can be determined by using D and rounding it up to the largest integer as follows:

$$num = \text{roundup}(\frac{A_s}{\pi D^2/4}) \tag{12}$$

Throughout this paper, the rebar diameter (D) can vary.

Now that the geometry of the beam is defined, the crack depths $\{cd\}$ for the beam with num to 1 rebars can be calculated.

3.2 Calculate crack depths (B)

The concrete crack is to the depth of the NA. The NA is calculated using Equation 4. The crack depth is calculated for each case of the beam having num to 1 rebars. All calculated crack depths are stored in a vector $\{cd\}$. $\{cd\}$ is used next to calculate the stresses in the rebars.

3.3 Calculate stresses (C)

The stress (σ_s) in the rebars is calculated using the transformed-section method as explained by Hibbeler (2008) p. 340.

The stress is calculated using,

$$\sigma_s' = \frac{M_{max}(cd_i - y_2)}{I_{tot}} \tag{13}$$

and then re-adjusted using,

$$\sigma_s = \frac{E_s}{E_c}\sigma_s' \tag{14}$$

cd_i is also used when calculating the second moment of area (I_{tot}). The stress is calculated for each case of the beam having num to 1 rebars and stored in a vector $\{\sigma\}$.

3.4 Monte Carlo simulation (D)

A number of the variables used to generate the P-F curve are stochastic in nature, most importantly the rebar S-N curve properties. A Monte Carlo simulation allows one to calculate the variability of the outcome of a model that is subject to statistical uncertainty and variability of its inputs. In the present case, such a simulation entails repeating the process of generating the cycles to failure $\{n\}$, where the stochastic input variables are randomly selected for each iteration, based on their respective probability distributions. The combination of all iterations gives a distribution of cycles to failure $[n]$.

The Monte Carlo simulation repeats step E to H in Figure 7 many times. From this set of cycles to failure $[n]$, it is then possible to again define a single cycles to failure $\{n\}_{conf}$ but at a chosen confidence level k. The confidence level k may also be interpreted as the probability that the beam would have a longer life than what is indicated by this cycles to failure $\{n\}_{conf}$, in other words, the risk of the result being non-conservative, or the certainty that the result is conservative.

The simulation becomes more accurate as more iterations are run (or the larger mc is). However, more iterations mean more computation time. In some circumstances, probabilities of failure of one in tens of thousands or even millions would be of interest, especially if the consequence of failure implies a cost which is orders of magnitude larger than the repair cost. In such cases, accurate computation of the failure probability would require a very high number of Monte Carlo simulations and therefore application of advanced Monte Carlo techniques (Pedroni et al. (2017)). In the present study, such accuracy is not required. But the method could easily be extended to employ these advanced techniques.

The steps within the Monte Carlo simulation are explained next. The output of the simulation is a set of cycles to failure $[n]$.

3.4.1 Assign probability of failure (E)

A vector with random probabilities between 0 and 1 of length num is created $\{prob\}$. $\{prob\}$ is then sorted from small to large. $prob_1$ is the probability of the first rebar to fracture.

3.4.2 Calculate cycles to failure (F)

A vector with the cycles to failure $\{n\}$ of each rebar is then calculated. The sum of $\{n\}$ is the number of cycles to failure for the entire beam. $\{n\}$ is calculated by following steps G and H.

CDF (G) The experimental results of Tilly (1979) are used to get a failure distribution of a rebar at the corresponding stress σ_i. Figure 8 shows the authors' replication of Tilly's S-N curve.

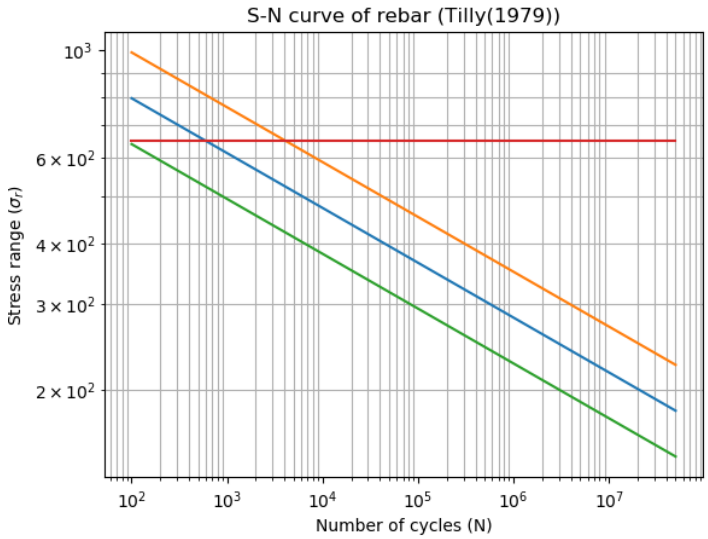

Figure 8: The Authors' replication of Tilly's S-N Curve for RC beams.

A cumulative distribution function (CDF) for each stress σ_i is calculated. The CDF is used to assign the cycles to failure for the randomly generated probabilities. For example, if a probability of 0.3 was generated, the cycles to failure at 257 MPa would be 1 000 000 cycles as shown in Figure 9. However, if the stress is higher than the ultimate tensile strength the cycles are taken as 1.

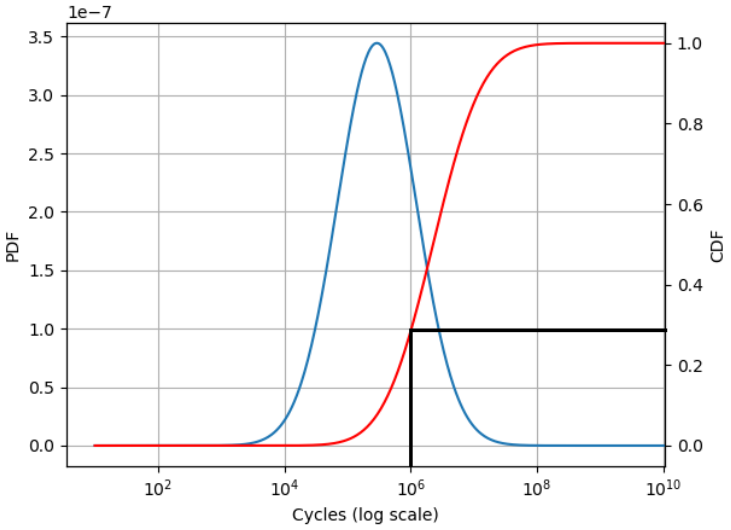

Figure 9: The PDF and CDF created from Tilly's S-N curve at a single stress of 257 MPa.

A matrix $[N]$ is therefore created for each stress in $\{\sigma\}$ at all probabilities in $\{prob\}$. N_{ij} is the

number of cycles to failure of the j^{th} rebar at the i^{th} stress. For example, N_{12} is the number of cycles to failure of the 2nd rebar ($prob_2$) at the 1st stress (σ_1).

Calculate cycles to failure (H) The Palmgren-Miner law of damage accumulation (Palmgren (1924) & Miner (1945)) is used to calculate the number of cycles to failure of each rebar (n_i).

The stress cycles experienced by the 1st (n_1), 2nd (n_2) and 3rd (n_3) rebar in a beam with 4 rebars to fail are shown in Figure 10.

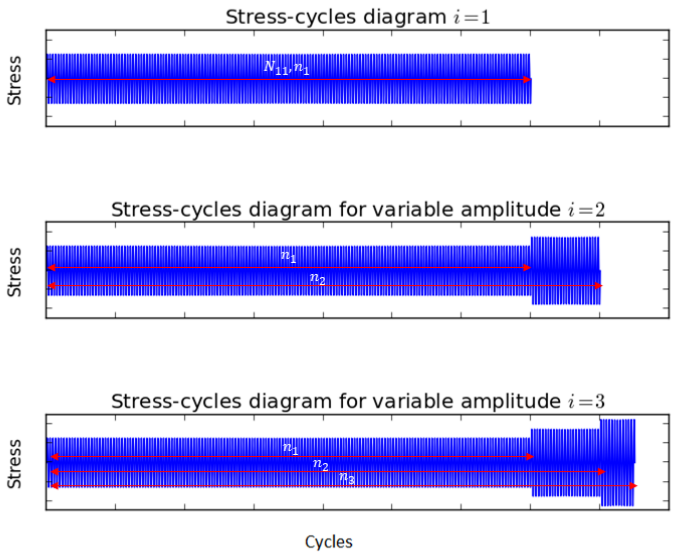

Figure 10: Stress-cycles diagrams for rebar 1,2 and 3

The top plot shows the life of the 1st rebar to failure. This rebar experiences only one stress range up until its failure. The 2nd rebar, however, experiences the same number of cycles at the same stress range as the 1st rebar, and after the 1st rebars fails, experiences a higher stress range up until its failure as shown in the middle plot. The 3rd rebar experiences the same number of cycles at the same 2 stress ranges as the 2nd rebar, and after the 2nd rebar fails, experiences an even higher stress range up until its failure as shown in the bottom plot. This process repeats, depending on the number of rebars.

Each rebar accumulates a certain amount of damage during the cycles that led to the preceding rebar failures. The number of cycles to failure of each respective rebar, while considering the effect of this accumulated damage, can be calculated with the help of the Palmgren-Miner law.

Equations 15, 16, 17 and 18 represent the Palmgren-Miner law for failure of the 1st, 2nd, 3rd and 4th rebar, respectively.

$$\frac{n_1}{N_{11}} = 1 \tag{15}$$

$$\frac{n_1}{N_{12}} + \frac{n_2 - n_1}{N_{22}} = 1 \tag{16}$$

$$\frac{n_1}{N_{13}} + \frac{n_2 - n_1}{N_{23}} + \frac{n_3 - n_2}{N_{33}} = 1 \tag{17}$$

$$\frac{n_1}{N_{14}} + \frac{n_2 - n_1}{N_{24}} + \frac{n_3 - n_2}{N_{34}} + \frac{n_4 - n_3}{N_{44}} = 1 \tag{18}$$

Where, n_i is the number of cycles to failure of the ith rebar i.e. n_1 is the number of cycles to failure of the 1st rebar.

Rearranging each equation to give the cycles to failure of each rebar:

$$n_1 = N_{11} \tag{19}$$

$$n_2 = n_1 + N_{22}\left(1 - \frac{n_1}{N_{12}}\right) \tag{20}$$

$$n_3 = n_2 + N_{33}\left(1 - \frac{n_1}{N_{13}} - \frac{n_2 - n_1}{N_{23}}\right) \tag{21}$$

$$n_4 = n_3 + N_{44}\left(1 - \frac{n_1}{N_{14}} - \frac{n_2 - n_1}{N_{24}} - \frac{n_3 - n_2}{N_{34}}\right) \tag{22}$$

A generalised expression is given by:

$$n_i = n_{i-1} + N_{ii}\left(1 - \frac{n_1}{N_{1i}} - \left(\sum_{j=1}^{i-1} \frac{n_{j+1} - n_j}{N_{ji}}\right)\right) \tag{23}$$

With:

$$n_1 = N_{11} \tag{24}$$

n_i Number of cycles to failure of the i^{th} rebar. Starting i from 2.
N_{ij} Number of cycles to failure of the j^{th} rebar at the i^{th} stress.

3.5 Determine confidence-interval cycles to failure (I)

The part of the P-F curve that we are interested in is the P-F interval (between failure of the first rebar (n_1) and total failure of the beam (n_{num})). The output of the Monte Carlo simulation is a set of cycles to failure:

$$[N] = \left[\{n\}_1, \{n\}_2, \{n\}_3, ..., \{n\}_j\right] \tag{25}$$

A probability distribution can now be created for the remaining life of the second rebar after the first rebar has failed ($n_2 - n_1$), third rebar after the second rebar has failed ($n_3 - n_2$), etc. Each one of these probability distributions has a corresponding CDF curve.

Figure 11 shows $n_2 - n_1$ for 500 randomly generated beams: a Weibull distribution was fitted over these results which yielded a Weibull shape parameter of $k = 1$, therefore the Weibull takes the shape of an exponential distribution, and scale parameter of $\lambda = 136229$. The CDF of this Weibull density function is shown in Figure 12.

Now, a *single* cycles to failure vector $\{n\}_{conf}$ is made from the results by using the chosen certainty/confidence of avoiding failure. $\{n\}_{conf}$ is the x-axis of the PF-curve. If the beam

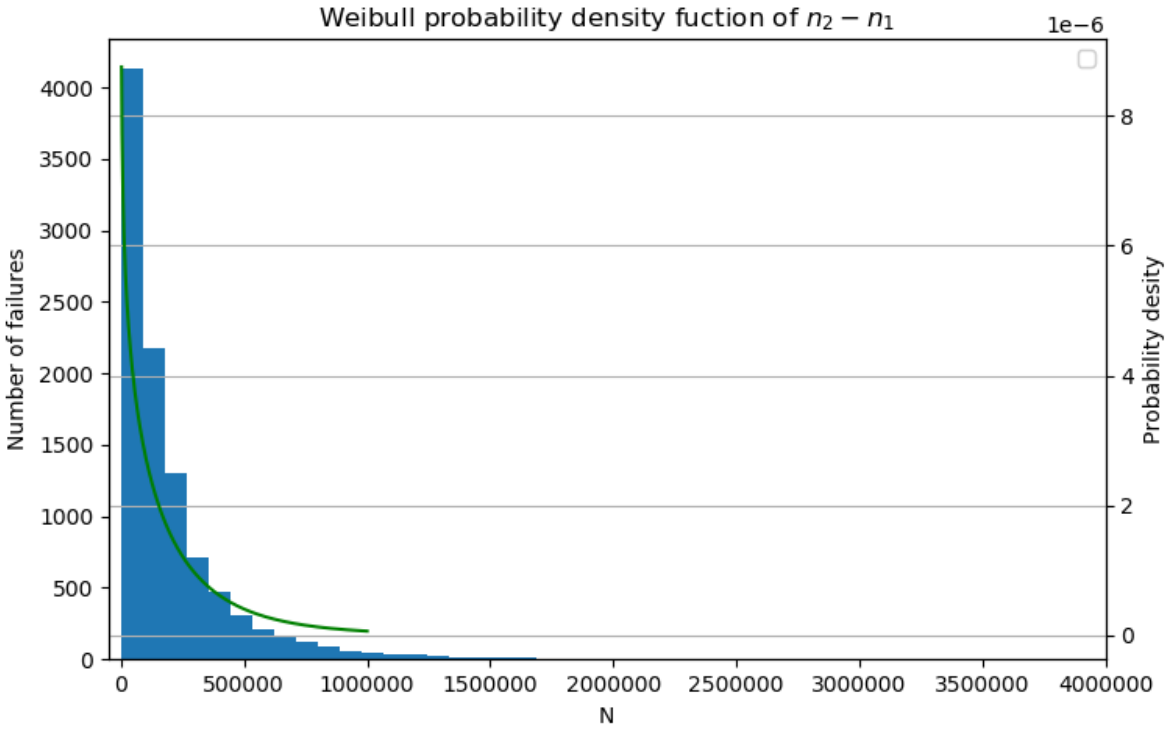

Figure 11: Weibull probability density function (line) and number of failures (bars) of $n_2 - n_1$

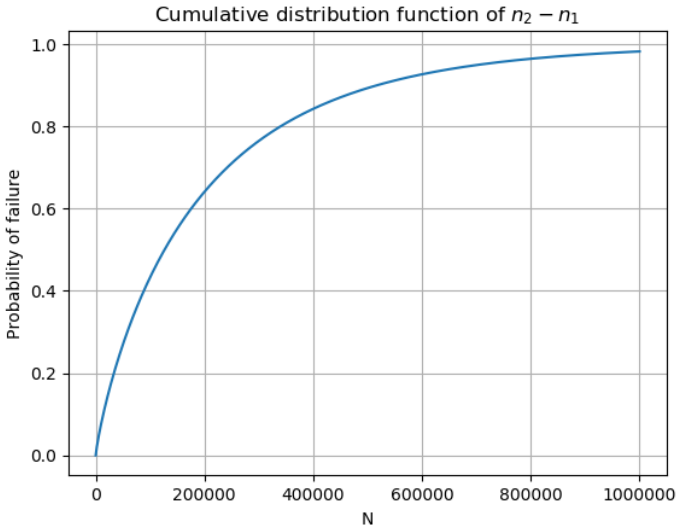

Figure 12: Cumulative distribution function of $n_2 - n_1$

in question is a critical beam, a high certainty of for example 90% would be desired to avoid failure so the chosen certainty that will be used in the CFD could be $\frac{100-90}{100} = 0.1$.

3.6 Determine condition (J)

The earlier determined $\{cd\}$ is used to calculate another vector $\{cond\}$ that is the y-axis of the P-F curve (condition):

$$cond_i = \frac{cd_i}{h} \tag{26}$$

Combining $\{cond\}$ (y-axis) and $\{n\}_{conf}$ (x-axis), a P-F curve is created.

4 Using the model

Consider a plant that has a RC beam that is subjected to fatigue that has parameters as shown in Table 2. During a structural inspection, flexural concrete cracks were found in the beam that are cracked to the depth of the neutral axis. It will now be demonstrated how the proposed model can be used in this case to help make a decision.

Parameter		**Value**
Length	(L)	1 m
Height	(h)	0.19 m
Breadth	(b)	0.08 m
Concrete strength	(σ_{yc})	40 MPa
Steel strength	(σ_{ys})	400 MPa
Number of rebars	(num)	4
Rebar diameter	(D)	0.008 m
Load	(P)	1 t
Load span	(s)	0.2 m
Frequency of load	(f)	17 minutes/cycle (98×10^{-3} Hz)

Table 2: Plant RC beam parameters

The financial consequence of failure and the cost of mitigation are as shown in Table 3. The consequence of failure consists of repair of any machines that are contained inside the structure, the standing time cost, and the cost to repair the beam. The mitigation only includes cost of beam repair.

The mitigation costs is $\frac{\text{R20 million}}{\text{R200 million}} = 10\%$ of the consequence cost.

A risk-based approach can be followed to calculate the *confidence level* that should be used during the Monte Carlo part of the model. Risk is defined as probability $\times$ consequence. The risk of failure at 10% probability (or 90% confidence level) is therefore:

$$0.1 \times 200 \text{ million} = \text{R20 million} \tag{27}$$

This is the cost of mitigation.

If the confidence level is chosen lower than 90%, the expected cost of failure will be higher than the mitigation cost, and vice versa if the confidence level is chosen higher than 90%. Therefore, **90%** is the optimal confidence level to use in the Monte Carlo simulation.

Since the rebar area and number of rebars are known, the design part of the model can be skipped. Figure 13 shows the result of applying the proposed model to this beam with the

Consequence	
Repair machines	R60 million
Standing time (days)	4 days
Standing time (shifts)	8 Shifts
Standing cost per shift	R15 million
Standing cost	R120 million
Repair beam	R20 million
Consequence of failure:	**R200 million**
Mitigation	
Repair beam	R20 million
Mitigation cost:	**R20 million**

Table 3: Consequence and mitigation cost

above parameters, with 90% confidence of avoiding failure. Tilly's S-N curve was used to get the cycles to failure for the baseline beam. n_1 was set to an arbitrary value of 20 000, the reason being that the interval of interest is after the first rebar failure. How long it takes to get to this point is not of interest.

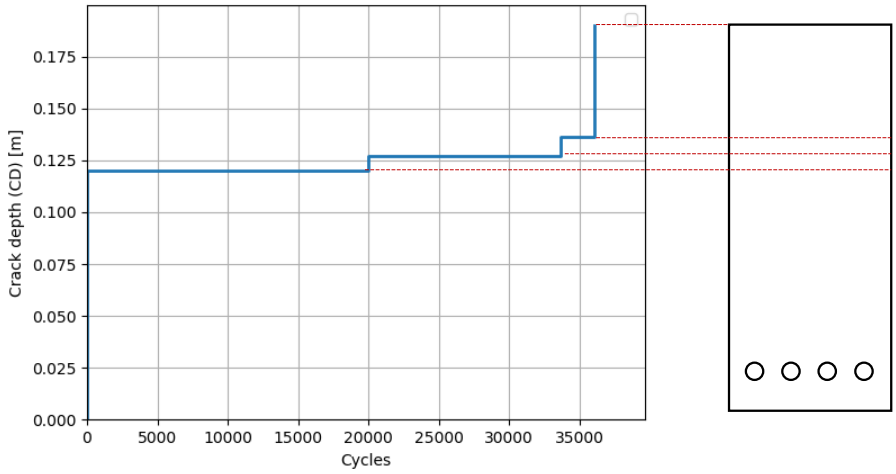

Figure 13: Baseline crack growth curve that is used for comparison in the numerical results

The figure shows that with 90% confidence level, we can expect the second rebar to survive at least 14 000 cycles after the 1st one failed. With a frequency of 17 min/cycle, the number of days between first and second rebar failure is calculated as,

$$n_2 - n_1 = 14\,000 \text{ cycles} \tag{28}$$
$$= 14\,000 \times \tfrac{17}{1440} \text{ days} \tag{29}$$
$$= 165 \text{ days} \tag{30}$$

And, when the first rebar fails, the crack will grow with 8 mm.

Knowing that we are at some point before any rebar has failed, the beam can be inspected every day until the cracks grow 8 mm. When this happens, the beam should be repaired before the elapse of 165 days to balance the risk.

5 Numerical Experiments

In this section, the effects of changing numerous variables in the model were investigated. Each variable was changed, while keeping everything else the same, and every result is plotted next to or together with a baseline curve to make comparison possible. In most cases, the variables were changed to a relatively extreme value, to see a significant difference. The impact that every result will have on the above mentioned case will also be discussed. Figure 13 is the baseline crack growth curve to which all results will be compared.

Firstly, the effects of changing the certainty are presented. Then, the effects of changing design variables (i.e. the beam height, breadth, steel and concrete strength), using a different S-N curve and changing the number of rebars are shown. n_1 of each result was also set to an arbitrary value of 20 000 as with the baseline curve for the same reason.

5.1 Effect of different certainties

A higher certainty is more conservative, so the model would predict that the failure would happen sooner to avoid failure. A more conservative certainty would be chosen for a beam with a higher consequence of failure to reduce the risk. For example in the case of the beam in the above example, if the consequence cost was R300 million and the mitigation cost was the same, the chosen certainty should be $1 - \frac{\text{R20 million}}{\text{R300 million}} = 93.3\%$.

As one would expect, a higher chosen certainty gives lower cycles to failure as shown in Figure 14. Chosen certainties of 90% and 93.3% give ±14 000 and ±8 300 cycles, respectively. 8 300 cycles is 98 days for the given loading frequency. This is still sufficient time to plan and schedule a repair of the beam. The beam can confidently be used until then, providing extended life.

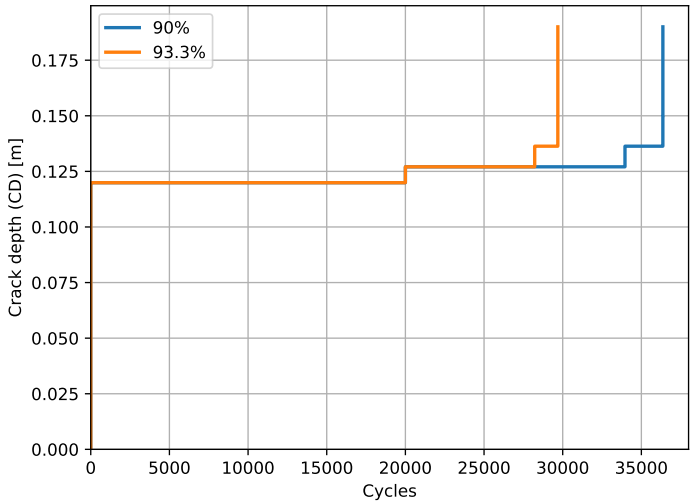

Figure 14: Comparison of different certainties

5.2 Effect of changing design variables

In this section, 4 different design variables were respectively changed; beam height (h), beam breadth (b), concrete strength (σ_{yc}) and steel strength (σ_{ys}).

5.2.1 Beam height (h)

If the resultant crack growth curve of a very *tall* beam is compared to the baseline, it can be seen that the life of the taller beam ($n_2 - n_1 = 5800$ cycles $= 68$ days) is less than the baseline (see Figure 15). This is because the stresses in the rebars are greater for the taller beam (for the baseline beam $\sigma_0 = 240$ MPa and $\sigma_0 = 260$ MPa for the tall beam), thus, the S-N curve would give fewer cycles to failure.

The change in crack depth per rebar failure is, however, slightly more for the taller beam (10 mm as compared to 8 mm). This is more desirable because a rebar failure would then be more detectable.

The design gives the rebar diameter of the tall beam to be 3 mm.

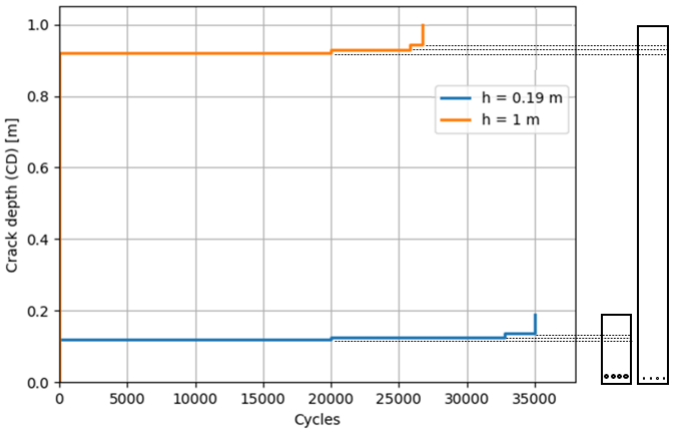

Figure 15: Comparison of different beam heights

5.2.2 Beam breadth (b)

If the resultant crack growth curve of a very *wide* beam is compared to the baseline, it can be seen that the life of the wider beam ($n_2 - n_1 = 6250$ cycles $= 74$ days) is less than the baseline (see Figure 16). This is because the stresses in the rebars are greater for the wider beam (for the baseline beam $\sigma_0 = 240$MPa and $\sigma_0 = 264$MPa for the wide beam), thus, the S-N curve would give fewer cycles to failure.

The change in crack depth per rebar failure is, however, significantly less for the wide beam (2.5 mm as compared to 8 mm). This is not desirable because a rebar failure would be difficult to detect.

The design gives the rebar diameter of the wide beam to be 8 mm.

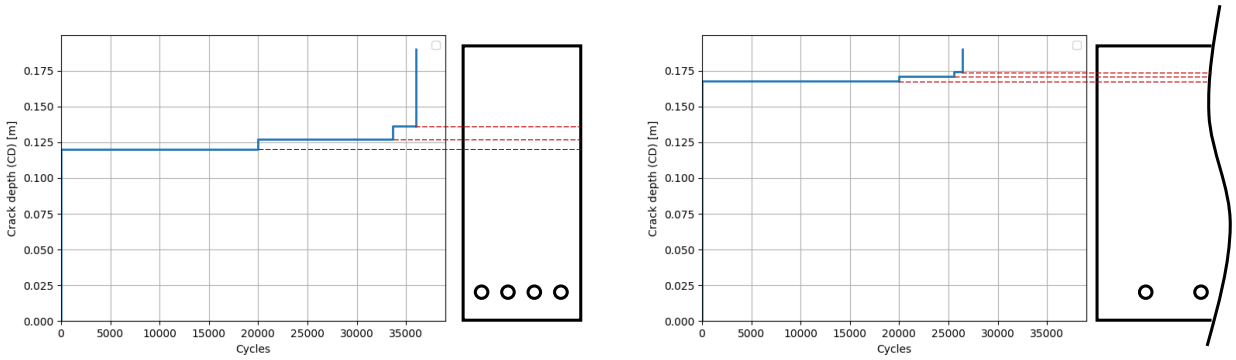

Figure 16: Comparison of different beam widths

5.2.3 Steel strength (σ_{ys})

If the resultant crack growth curve of a beam with a lower steel strength is compared to the baseline, it can be seen that the life is more for the lower steel strength (see Figure 17). This is counter-intuitive because one would expect the life of the beam to be higher for higher strength steel.

In reality, the strength of the steel is a design input *and* deterministic in the S-N curve. In this case, the strength of the steel was only changed as a design input and the S-N curve was kept the same.

The lower steel strength ends up giving a higher life because lower steel strength will require a larger steel area (A_s) to ensure that the stress will be lower in the steel. Higher A_s will cause a bigger D. Lower stress in the steel will give higher number of cycles from the S-N curve. The effect of changing the S-N curve is investigated later in this chapter in a separate section.

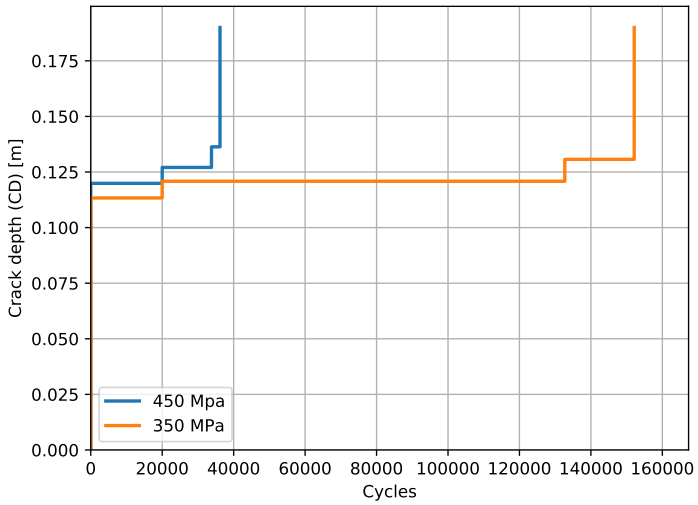

Figure 17: Comparison of different steel strengths

5.2.4 Concrete strength (σ_{yc})

If the resultant crack growth curve of a beam with a lower concrete strength is compared to the baseline, it can be seen that the life is more for the lower concrete strength (see Figure 18).

This is because of the same reason as with the lower steel strength i.e. a lower concrete strength will require a larger steel area (A_s) to ensure that the stress will be lower in the concrete. Higher A_s will cause a bigger D. Lower stress in the steel will give higher number of cycles from the S-N curve. The effect of changing the S-N curve is investigated later in this chapter.

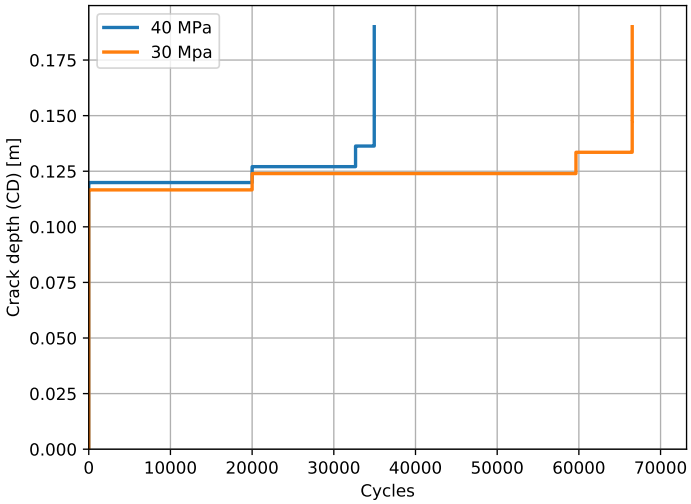

Figure 18: Comparison of different concrete strengths

5.3 Effect of different S-N curves

In this section, the S-N curve is changed in 2 ways. Firstly, the shape is changed to be narrow and then wide by changing the standard deviation (st. dev or SD), and secondly, the position of the mean is moved up.

5.3.1 S-N shape

The equation for the mean line of Tilly's S-N curve is:

$$\log N = \log 27.7 - 8.858 \log \sigma \tag{31}$$

And the equation for the top 95.45 percentile line is:

$$\log N = \log 27.7 - 8.858 \log \sigma + 2 \times SD \tag{32}$$

In the case of Tilly's S-N curve, $SD = 0.0472$. To achieve a narrow shape as shown in Figure 19a, SD is changed to 0.01, and to get a wide shape as shown in Figure 19b, SD is changed to 0.1.

Figure 20 shows the results of changing the shape of the S-N curve. The life of the beam is greater for a S-N curve with a narrow shape. This is because the shape of the S-N curve, ultimately, determines the shape of the distribution of $n_{k+1} - n_k$. Then, when the certainty is chosen (in this case 10%), the cycles will be greater because the certainty will be closer to the mean.

The life of the beam is less for a S-N curve with a wide shape. Following a similar reasoning as with the narrow shape: the S-N curve, ultimately, determines the shape of the distribution of $n_{k+1} - n_k$. Then, when the certainty is chosen, the cycles will be lower because the certainty will be further away from the mean.

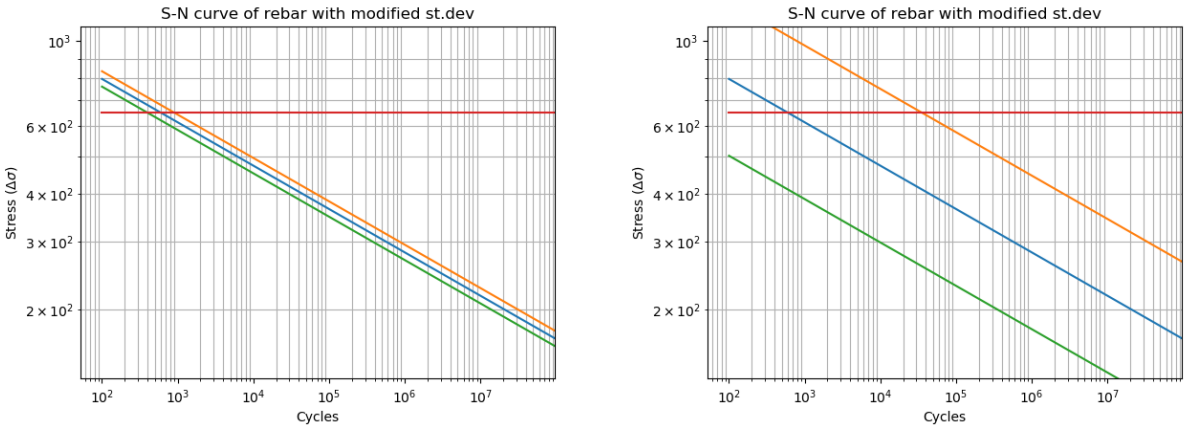

(a) S-N curve with a narrow shape ($SD = 0.01$) (b) S-N curve with a wide shape ($SD = 0.1$)

Figure 19: S-N curve with different shapes

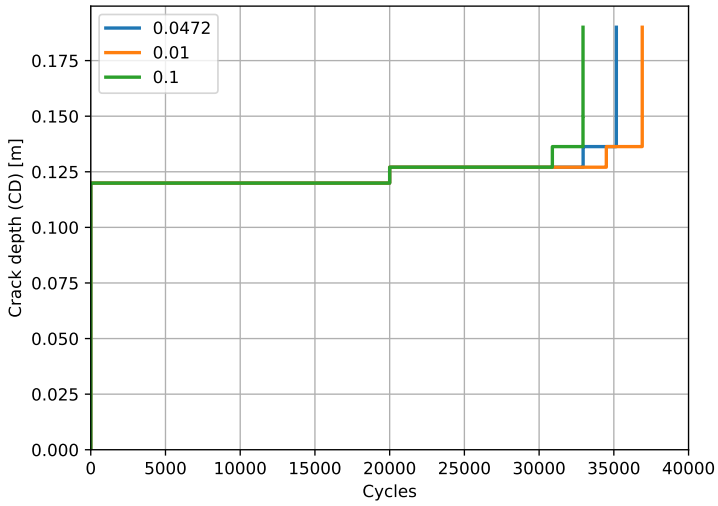

Figure 20: Comparison of different S-N curve shapes

5.3.2 S-N position & slope

The effect of changing the position & slope of the S-N curve was investigated. The S-N curve was adjusted as shown in Figure 21b. The original S-N curve is also shown on the left to make the comparison easier.

The equation for the mean line was changed to the equation given by BS 7608 (2014):

$$\log N = \log 14.0342 - 3.5 \log \sigma \tag{33}$$

And the equation for the top 95.45 percentile line was changed to:

$$\log N = \log 14.0342 - 3.5 \log \sigma + 2 \times SD \tag{34}$$

The crack growth curves for the different S-N curves are shown in Figure 22 and differ only slightly. $n_2 - n_1$ for Tilly's S-N curve is greater as compared to BS 7608 (2014). This is because the slope of Tilly's curve is flatter so at low stresses, the cycles are great, but quickly becomes few at high stresses. The slope of BS 7608 (2014) is steep so it will give relatively few cycles

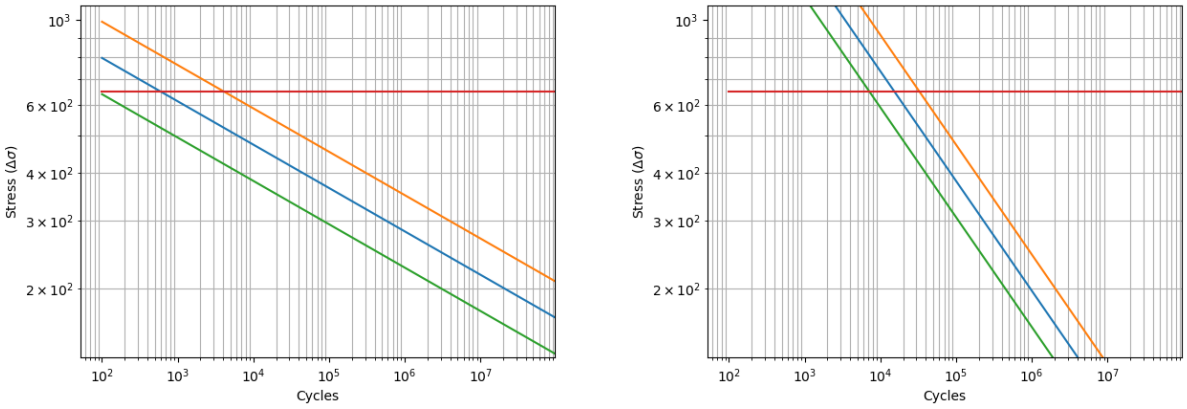

(a) Tilly's S-N curve (b) BS 7608 (2014) S-N curve

Figure 21: S-N curves with different position

at low stresses, but will not change too quickly when the stresses increase so $n_3 - n_2$ is greater for BS 7608 (2014) as compared to Tilly.

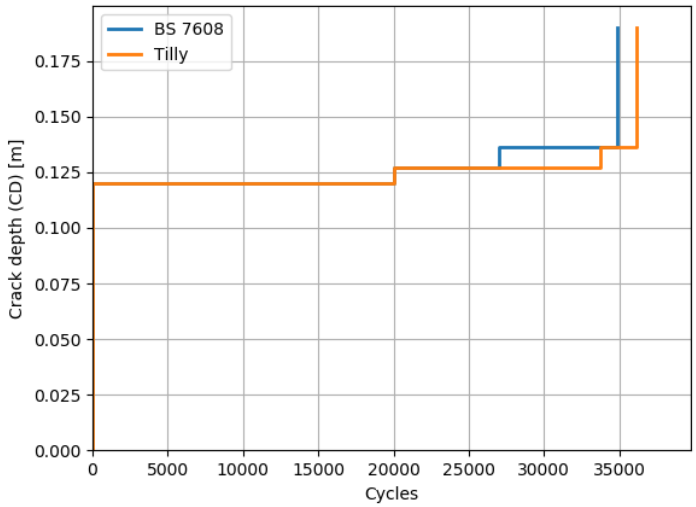

Figure 22: Comparison of different S-N curve shapes

5.4 Effect of number of rebars

In this section, the number of rebars were changed. Firstly, the number of rebars were changed, but the steel area given by the design (A_s) was kept constant. Secondly, the number of rebars were changed by adding an extra rebar i.e. increasing A_s.

5.4.1 Number of rebars: constant area

The effect of the number of rebars on the life of the beam was investigated, while the rebar area given by the design (A_s) were kept constant. 4 scenarios were modelled: 2, 4, 7 and 12 rebars. The rebar diameter decreases with more rebars. The design gave the rebar diameters to be 12,

8, 6.5 and 5 mm for 2, 4, 7 and 12 rebars, respectively. Figure 23 shows the section views of these 4 beams.

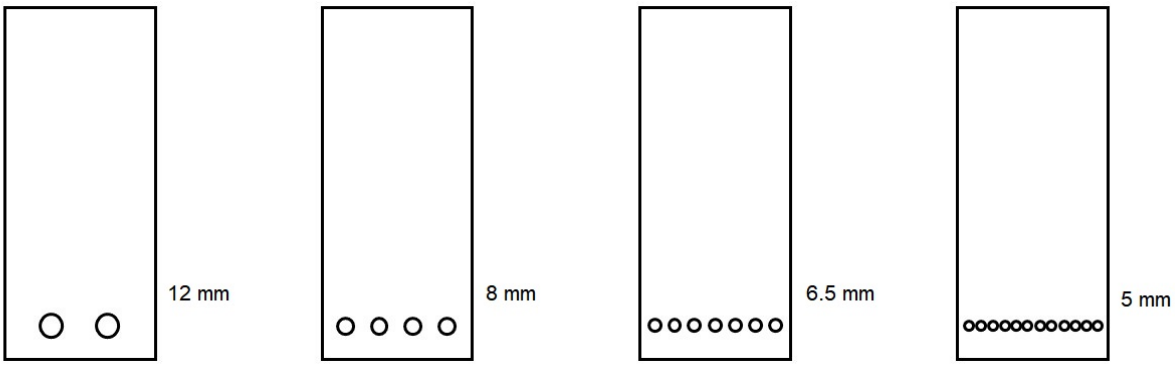

Figure 23: Section views of the beams with 2, 4, 7 and 12 rebars

Figure 24 shows the resultant crack growth curves of beams with 2, 4, 7 and 12 rebars. The total life of the beam is increased, if more rebars are present. This is because if one rebar fails for a beam with many rebars, the steel area only decreases by a bit, causing the neutral axis to only move up a bit. The stress increase per rebar failure is thus small, and small stress means more cycles.

However, the detectability per rebar failure, decreases with more/smaller rebars. More rebars give longer beam life, but failure of a single rebar will be more undetectable. This is easily overcome by not trying to detect number of rebar failures, but by looking at crack depth. $n_2 - n_1$ could be undetectable, but $n_3 - n_1$ or $n_4 - n_1$ could be detectable.

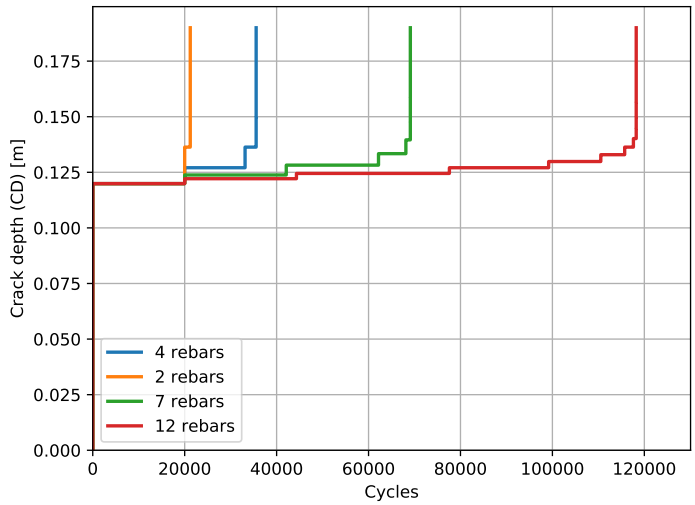

Figure 24: Crack growth curve of beams with 2, 4, 7 and 12 rebars

5.4.2 Number of rebars: constant diameter

The effect of the number of rebars on the life of the beam was investigated, by adding an additional rebar. The beam is thus over-designed because the rebar area is forced to be higher than the design. Figure 25 shows the section view of the baseline beam, with 4×8 mm rebars, and the beam with an extra rebar.

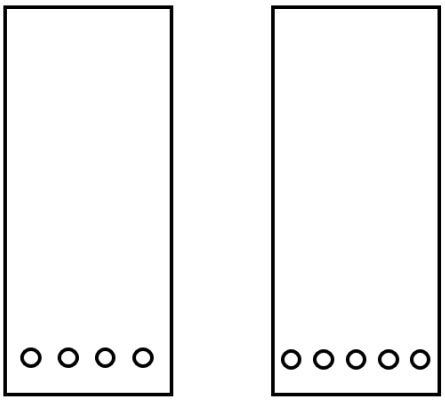

Figure 25: Section views of beams with 4 and 5 rebars

As one would expect, the life of the beam increases with the over-designed beam because the stresses in the rebars are lower. Figure 26 show the resultant crack growth curves of these 2 beams.

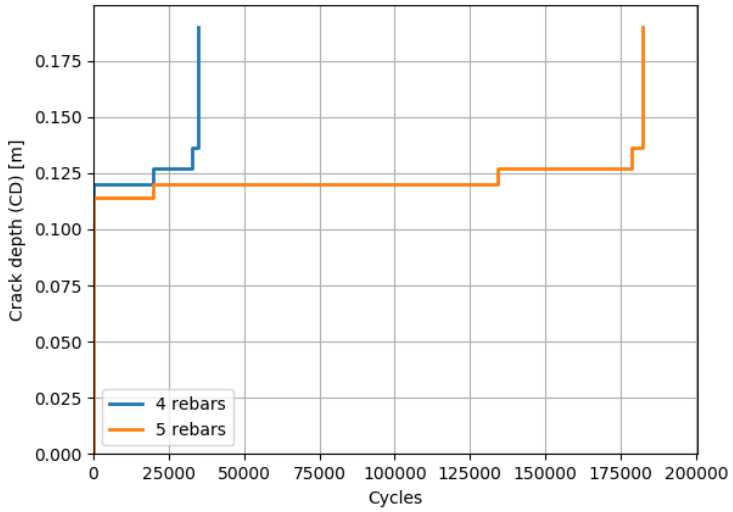

Figure 26: Crack growth curve of beams with 4 and 5 rebars

5.5 Interpretation of results

This section discusses how certain results from the numerical experiments can give guidance to making design decisions when designing a RC beam that will be subjected to fatigue.

The model predicts that wider beams will have shorter life spans and a less detectable crack growth. This is not desirable in any way, so the conclusion that can be drawn is that wide beams should be avoided during design for fatigue. On the other hand, the model predicts that taller beams will have a more detectable crack growth, but shorter life span. So during the design, the beams should be designed to be just tall enough so the crack would be detectable with whichever method is used.

The model shows that the number of rebars with constant area have benefit for fatigue life of the beam and has implications on detectability of the crack growth i.e. more rebars means smoother external crack growth. This could be used in a similar way as the leak-before-break

design strategy.

In structures containing a fluid such as pipes or pressure vessels, fracture mechanics principles can be used during the design to ensure a flaw will develop through the wall that will leak before catastrophic rupture occurs (Bourga et al., 2015). In case of leak-before-break, decisions are made during the design phase for the benefit of ensuring detectability during in service maintenance.

6 Conclusion

In this study, a model to create a P-F curve based on flexural concrete crack depths is developed for beams that are subjected to high-cycle cyclical loading. The model is developed using rebar fatigue test results from Tilly 1979 and the Palmgren-Miner law of damage accumulation. The model includes randomly sampling from a distribution. A Monte Carlo simulation with statistical distributions is employed to provide confidence levels of RUL outputs.

By means of an example, it is shown how repair decisions for a RC beam found in a plant that has flexural cracks can be made based on this predicted RUL. For the example given, the model predicts with 90% confidence that the second rebar will survive 165 days after the first rebar fractures. This section proves that the model can be used in practise and provides concrete actions for management of a plant to take.

A sensitivity study is then performed to show the effect that different chosen certainties, design variables, S-N curve, and number of rebars would have on the output of the model. Some of the findings are listed below:

- A tall beam would have a lower fatigue life, but would have a more detectable change in condition
- A wide beam is undesirable, because it would have a lower fatigue life and a less detectable change in condition
- Lower steel strength gave the counter intuitive result of higher fatigue life. This was found to be because the steel strength is only changed as a design input and not in the S-N curve.
- The S-N curve that is used is shown to affect the output greatly, so it is important to use the correct S-N curve or, at least, a conservative one.
- More rebars (but with the same steel area) were found to be more desirable because it increases the fatigue life and gives more and smaller incidence of crack growth.

In this study, the model was conceptualised and tested analytically and stochastically. However, physical tests and/or accurate finite element analysis would be necessary to establish further confidence in the model, for instance in how the crack grows over the section of the beam when a rebar fails.

References

Blann, D. R. (2013). Maximizing the P-F Interval Through Condition-Based Maintenance.

Bourga, R., Moore, P., Janin, Y. J., Wang, B., & Sharples, J. (2015). Leak-before-break: Global perspectives and procedures. *International Journal of Pressure Vessels and Piping*, *129*, 43–49.

BS 7608 (2014). Guide to fatigue design and assessment of steel products. Technical report.

BS 8110-1 (1997). Structural use of concrete — Part 1: Code of practice for design and construction. Technical report.

Campbell, J. D. & Reyes-Picknell, J. V. (2015). *Strategies for Excellence in Maintenance Management* (3rd ed.).

Carino, N. J. & Clifton, J. R. (1995). Prediction of Cracking in Reinforced Concrete Structures. *National Institue of Standards and Technology*, 49.

Chen, H. P. & Alani, A. M. (2013). Optimized maintenance strategy for concrete structures affected by cracking due to reinforcement corrosion. *ACI Structural Journal*, *110*(2), 229–238.

Guo, Z. (2014). *Principles of Reinforced Concrete Design*. Oxford: Elsevier Inc.

Guo, Z., Ma, Y., Wang, L., & Zhang, J. (2019). Modelling guidelines for corrosion-fatigue life prediction of concrete bridges: Considering corrosion pit as a notch or crack. *Engineering Failure Analysis*, *105*(November 2018), 883–895.

Helgason, T., Hanson, J. M., Somes, N. F., Corley, W. G., & Hognestad, E. (1976). Fatigue strength of high-yield reinforcing bars. Technical report, WASHINGTON D.C.

Hibbeler, R. C. (2008). *Mechanics of Materials* (7th ed.). Prentice Hall.

Japan Society of Civil Engineers (2007). Standard Specification for Concrete Structures "Maintenance".

Jokubaitis, V., Juknevičius, L., & Šalna, R. (2013). Conditions for failure of normal section in flexural reinforced concrete beams of rectangular cross-section. *Procedia Engineering*, *57*, 466–472.

Lee, M. K. & Barr, B. I. G. (2004). An overview of the fatigue behaviour of plain and fibre reinforced concrete. *Cement and Concrete Composites*, *26*(4), 299–305.

Miner, M. (1945). Culmulative Damage in Fatigue, Trgins. *ASME J. Applied Mechanics*, *12*, 2.

Mosley, W. H. & Bungey, J. H. (1990). *Reinforced concrete design* (4th ed.). London: Macmillan education ltd.

Moubray, J. (1991). *Reliability-centred Maintenance*. Butterworth-Heinemann.

Nagesh, H. E. & Rao, G. A. (2016). Fatigue Behavior of Lightly Reinforced Concrete Beams in Flexure due to Overload. *Proceedings of the 9th International Conference on Fracture Mechanics of Concrete and Concrete Structures*.

Palmgren, A. (1924). Die Lebensdauer von Kugellagern. Z. VDI 68. *S339–S341*.

Papakonstantinou, C., Michael F., P., & Kent A., H. (2001). Fatigue behavior of RC beams strengthened with GFRP sheets. *Journal of Composites*, (November), 246–253.

Paris, P. C., Gomez, M. P., & Anderson, W. E. (1961). A rational analytic theory of fatiuge.

Pedroni, N., Zio, E., & Cadini, F. (2017). Advanced Monte Carlo Methods and Applications. *ASCE-ASME Journal of Risk and Uncertainty in Engineering Systems, Part A: Civil Engineering*, *3*(4), 02017001.

Prajapati, A., Bechtel, J., & Ganesan, S. (2012). Condition based maintenance: A survey. *Journal of Quality in Maintenance Engineering*, *18*(4), 384–400.

Pugno, N., Ciavarella, M., Cornetti, P., & Carpinteri, A. (2006). A generalized Paris' law for fatigue crack growth. *Journal of the Mechanics and Physics of Solids*, *54*(7), 1333–1349.

Rocha, M. & Brühwiler, E. (2012). Prediction of fatigue life of reinforced concrete bridges using Fracture Mechanics. *Bridge maintenance, safety, management, resilience and sustainability*, 3755–3760.

SABS 0100-1 (2000). THE STRUCTURAL USE OF CONCRETE - PART 1: DESIGN. Technical Report March, SOUTH AFRICAN BUREAU OF STANDARDS.

Tilly, G. & Moss, D. (1982). Long Endurance Fatigue of Steel Reinforcement. *IABSE Reports, International Association for Bridge and Structural engineering*, *37*, 229–238.

Tilly, G. P. (1979). FATIGUE OF STEEL REINFORCEMENT BARS IN CONCRETE : A REVIEW. *Fatigue of Engineering Materials and Structures*, *2*, 251–268.

Walraven, J. & Bigaj van Vliet, A. (2010). *The 2010 fib MODEL CODE FOR CONCRETE STRUCTURES: A NEW APPROACH IN STRUCTURAL ENGINEERING*.

Wang, W., Hussin, B., & Jefferis, T. (2012). A case study of condition based maintenance modelling based upon the oil analysis data of marine diesel engines using stochastic filtering. *International Journal of Production Economics TA - TT -*, *136*(1), 84–92.

Wessels, W. (2010). *Practical Reliability Engineering and Analysis for System Design and Life-Cycle Sustainment* (1st Editio ed.). CRC Press.

Yi, W.-j., Kunnath, S. K., Sun, X.-d., Shi, C.-j., & Tang, F.-j. (2011). Fatigue Behavior of Reinforced Concrete Beams with Corroded Steel Reinforcement. (107).